ELSEVIER

Journal of Magnetism and Magnetic Materials 151 (1995) 273–282

journal of magnetism and magnetic materials

Magnetic properties of the carbides Y_2ReC_2, Tb_2ReC_2, Er_2ReC_2 and Lu_2ReC_2

M. Reehuis [a], J. Rodriguez-Carvajal [b], M.E. Danebrock [c], W. Jeitschko [c,*]

[a] *Institut Laue–Langevin, BP 156, F-38042 Grenoble, France*
[b] *Laboratoire Léon Brillouin (CNRS-CEA), Centre d' Etudes de Saclay, F-91191 Gif-sur-Yvette Cedex, France*
[c] *Anorganisch-Chemisches Institut, Universität Münster, Wilhelm-Klemm-Str. 8, D-48149 Münster, Germany*

Received 24 January 1995; in revised form 3 April 1995

Abstract

Magnetic susceptibility measurements with a SQUID magnetometer reveal that the rhenium atoms in Y_2ReC_2 and Lu_2ReC_2 do not carry magnetic moments. The moments of the lanthanoid atoms in Tb_2ReC_2 and Er_2ReC_2 order antiferromagnetically below $T_N = 96(2)$ and 18(1) K, respectively. Both compounds show metamagnetic transitions, and above the Néel temperatures strong field-dependent paramagnetism was observed suggesting strong paramagnetic anisotropies. The antiferromagnetic structures of both compounds are different, however, with the same propagation vector $\boldsymbol{k} = 0$. They were determined from neutron powder data recorded in zero field at 1.5 K. The magnetic structures can be described with the basis functions [0, A_y, 0] and [G_x, A_y, A_z] for the terbium and erbium moments, respectively, using Bertaut's representation analysis.

1. Introduction

While there are numerous reports about the magnetic properties of the ferromagnetic rare-earth(R)–transition-metal carbides with the $Nd_2Fe_{14}B$, $Pr_2Mn_{17}C_3$ and $Tb_2Mn_{17}C_3$ type structures, where the transition-metal atoms carry magnetic moments [1–3], the magnetic properties of carbides with a higher content of carbon are less well known. However, in all of the few investigations describing the magnetic properties of such carbides the transition-metal atoms were found to be nonmagnetic, e.g. in the series $R_8Rh_5C_{12}$ [4], $RRhC_2$ [5], $RNiC_2$ [6], $R_7Ru_2C_{11}$ [7], $R_2Cr_2C_3$ [8], $R_4Ni_2C_5$ [9], $R_{10+x}Mn_{13-x}C_{18}$ [10], $RCoC_2$ [11] and RCoC [12], and thus the magnetic properties of these carbides are determined by the moments of the rare-earth–metal components. Their magnetic order was established only for some compounds of the series $RNiC_2$ and $RCoC_2$, where in the nickel containing compounds $TbNiC_2$ [13,14], $NdNiC_2$ [13,15], $TmNiC_2$ [13,15] and $ErNiC_2$ [13,16] the lanthanoid moments are ordered antiferromagnetically, whereas in $TbCoC_2$ [11], $DyCoC_2$ [17] and $HoCoC_2$ [17] these moments are ordered ferromagnetically. Only recently we have determined the magnetic structure of the antiferromagnet $Dy_2Cr_2C_3$ [18].

Here we report about the magnetic properties of some carbides R_2ReC_2 with a structure, which was first determined for Pr_2ReC_2 [19]. This compound contains a one-dimensionally infinite, anionic rhenium–carbon chain $_n[ReC_2]^{6n-}$. The band structure

* Corresponding author. Fax: +49-251-833146.

SSDI 0304-8853(95)00315-0

of this chain was investigated with extended Hückel calculations [20]. We find that only the rare-earth atoms of this orthorhombic compound carry magnetic moments. They occupy the Wyckoff site 4c of the space group Pnma with the site symmetry $\cdot m \cdot$.

2. Experimental details

The compounds were prepared by arc-melting cold-pressed pellets of the pure elements of the ideal composition. The stated purities were 99.9% for the metals and > 99.5% for the graphite flakes. For the annealing in evacuated silica tubes (2 weeks at 900°C) the samples were wrapped in tantalum foil. To dissolve some binary impurities, the powdered samples were treated with 1 m hydrochloric acid, washed with water and finally with ethanol. After this treatment the Guinier powder diagrams of the samples showed the patterns of the ternary carbides, frequently with a small impurity of nonmagnetic elemental rhenium.

The magnetic measurements were carried out with a SQUID magnetometer in the temperature range between 2 and 300 K and with magnetic flux densities of up to 5.5 T. Between 4 and 20 mg of the finely powdered samples were enclosed in thin-walled silica tubes of about 1 mm diameter. The samples were cooled in zero field down to 120 K for Tb_2ReC_2 and to 40 K for Er_2ReC_2, respectively, and either heated or cooled from these temperatures in the desired magnetic fields. In the case of the yttrium and lutetium containing compounds the samples were cooled down to 5 K and measured with increasing temperatures in applied flux densities of 3, 4 and 5 T up to room temperature.

The neutron powder diffraction measurements were carried out on the D1A instrument of the Institut Laue–Langevin (ILL) in Grenoble. During the reactor shutdown at the ILL this instrument was installed in the Orphée reactor (Laboratoire Léon Brillouin, Saclay). The D1A instrument uses germanium single crystals as monochromator with the 115 reflection giving a neutron wavelength $\lambda = 198.5$ pm. The Tb_2ReC_2 patterns were recorded at 1.5 and 150 K, the Er_2ReC_2 patterns at 1.5 and 30 K, both patterns at diffraction angles between $2\theta = 8°$ and 122.5°. The neutron powder diffraction data recorded

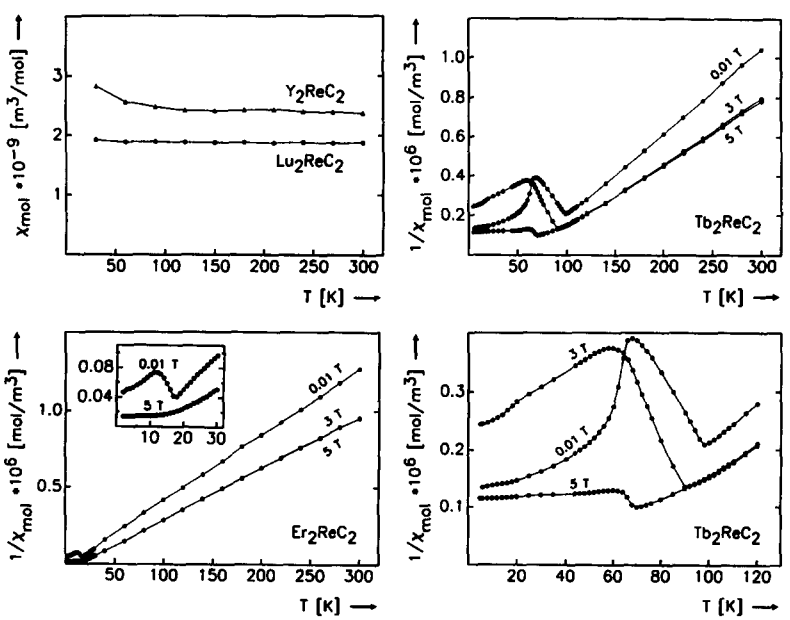

Fig. 1. Temperature dependence of the magnetic susceptibilities of Y_2ReC_2 and Lu_2ReC_2 and the reciprocal susceptibilities of Tb_2ReC_2 and Er_2ReC_2 obtained at different magnetic field strengths. For the yttrium and lutetium compounds, the susceptibilities were extrapolated to infinite field strengths. The inset gives an enlargement of the low temperature behaviour of Er_2ReC_2.

with $\lambda = 198.5$ pm had a rather poor counting statistics. However, the data were of sufficient quality to confirm the already known nuclear structure and to solve the magnetic structures. In the case of the terbium compound additional diffraction patterns were recorded at several temperatures (1.5, 50 and 80 K) in the 2θ range of 8–140°, using a wavelength of 311 pm from the 113 reflection of germanium, for which the flux is increased by a factor of five. The Rietveld refinements of the powder diffraction data were carried out with the program FULLPROF [21]. The nuclear scattering lengths used for the least-squares refinements were: b(Tb) = 7.38 fm, b(Er) = 8.03 fm, b(Re) = 9.2 fm and b(C) = 6.65 fm [22]. The dipolar approximations for the magnetic form factors of the rare-earth elements are available directly in the program FULLPROF. The coefficients to calculate the magnetic form factors in FULLPROF were obtained from Brown [23].

3. Results and discussion

The magnetic measurements (Fig. 1) show that the susceptibilities of Y_2ReC_2 and Lu_2ReC_2 are nearly temperature independent, indicating Pauli paramagnetism. At 300 K the susceptibility values of $\chi = 2.3 \times 10^{-9}$ m^3/mol and $\chi = 1.9 \times 10^{-9}$ m^3/mol were found for the yttrium and the lutetium compound, respectively. So the $[ReC_2]^{6-}$ polyanion does not carry localized magnetic moments. As discussed earlier [19], the electron configuration of the rhenium atoms is compatible with the 18-electron rule, and this is in good agreement with the Pauli paramagnetism of these compounds.

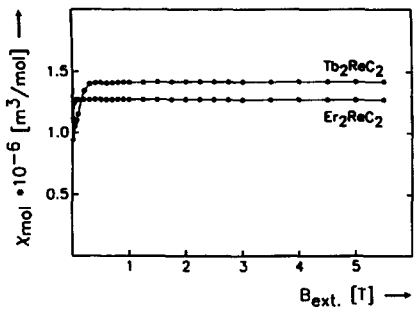

Fig. 2. Field dependence of the susceptibilities of Tb_2ReC_2 and Er_2ReC_2 at 300 K.

For Tb_2ReC_2 and Er_2ReC_2 the $1/\chi$ vs. T plots (Fig. 1) suggest antiferromagnetic ordering below 96(2) and 18(1) K, respectively. It can be seen that the Néel temperature of Tb_2ReC_2 is lowered from 96(2) K in a field of 0.01 T to 70(2) K at 5 T. The lowering of the Néel temperature with increasing external magnetic flux density is the expected behaviour of an antiferromagnet, while the Curie temperature of a ferromagnet is usually found to increase, when the external field is raised. Below 0.3 T (Tb_2ReC_2) and 0.1 T (Er_2ReC_2) the susceptibilities are field-dependent in the paramagnetic range (Fig. 2). This can be ascribed to a paramagnetic anisotropy as found for $PrRu_2Si_2$ [24–26]. For that reason the paramagnetic moments were calculated from the susceptibilities measured at 5 T. The paramagnetic moments, obtained from the $1/\chi$ vs. T plots (Fig. 1) are in good agreement with the theoretical values for the free Tb^{3+} and Er^{3+} ions (Table 1).

The magnetization of Er_2ReC_2 (Fig. 3) at 5 K shows a metamagnetic transition at the critical field strength $B = 0.9(1)$ T and reaches a magnetic mo-

Table 1
Magnetic properties of the carbides R_2ReC_2 (R = Y, Tb, Er, Lu). The experimental paramagnetic moments μ_{exp} obtained from $\mu_{exp} = 2.83\,[(\chi/2)\,(T-\Theta)]^{1/2}\ \mu_B$ are compared with the theoretical values $\mu_{eff} = g[J(J+1)]^{1/2}\ \mu_B$. The highest magnetic moments $\mu_{exp(sm)}$ reached in the magnetically ordered range of the powdered samples are listed together with the theoretical values $\mu_{calc(sm)}$ of the free R^{3+} ions where $\mu_{calc(sm)} = g\,J\,\mu_B$. The paramagnetic Curie temperatures Θ and the magnetic ordering temperatures T_N are also listed

Compound	Magnetic behaviour	μ_{exp} [μ_B/R^{3+}]	$\mu_{eff}(R^{3+})$ [μ_B]	Θ [K]	T_N [K]	$\mu_{exp(sm)}$ [μ_B/f.u.]	$\mu_{calc(sm)}$ [μ_B/f.u.]
Y_2ReC_2	Pauli-paramagnetic	–	0	–	–	–	0
Tb_2ReC_2	metamagnetic	9.7(2)	9.72	67(3)	96(2)	8.7	18.0
Er_2ReC_2	metamagnetic	9.6(2)	9.58	15(5)	18(2)	10.6	18.0
Lu_2ReC_2	Pauli-paramagnetic	–	0	–	–	–	0

ment of $\mu_{exp(sm)} = 10.6\mu_B$/f.u., which is considerably smaller than the theoretical value for two Er^{3+} ions, $\mu_{calc(sm)} = 2 \times 9.0\mu_B$. This difference can be attributed to the fact that the easy direction is not parallel to the applied magnetic field for all crystals of a powder sample. The critical field strength is decreasing slightly down to 0.5(1) T with increasing temperature up to 13 K (Fig. 3). In contrast, the metamagnetic transition of Tb_2ReC_2 is strongly temperature dependent. It occurs in one step in the curve recorded at 75 K and two steps are visible in the magnetization curves measured at 70 and 60 K (Fig. 3). The occurrence of this metamagnetism in two steps may be rationalized by the fact that there are two different terbium species, which turn their magnetic moments at different critical field strengths. Below 50 K the metamagnetic order can only be realized at magnetic field strengths higher than 5.5 T. At 70 K a magnetic moment of $\mu_{exp(sm)} = 8.7\mu_B$/f.u. was reached and this value is again significantly smaller than the theoretical value for two Tb^{3+} ions, $\mu_{calc(sm)} = 2 \times 9.0\mu_B$, probably for the same reason as discussed above for the erbium compound. Another possibility is that the metamagnetic transitions in these compounds are not complete for the magnetic fields available to us. The low value of the magnetic moment per f.u. could indicate the presence of an intermediate antiferromagnetic structure.

The nuclear structure (Fig. 4) of these carbides has already been determined from powder and single-crystal X-ray data of the compounds Ln_2ReC_2 (Ln = Pr, Er) [19]. The five different crystallographic sites (Ln1, Ln2, Re, C1 and C2) are all in the position 4c (x, $\frac{1}{4}$, z) of the space group Pnma. These structures were refined now also from neutron powder diffraction data (Fig. 5) taken at 150 K for Tb_2ReC_2 and at 30 K for Er_2ReC_2. A total of 25 variable parameters was refined: an overall scale factor, five peak shape parameters, the zero point, three lattice constants, the positional parameters x and z as well as the isotropic displacement parameters B of the five atomic sites. Additionally the two lattice constants and the overall scale factor of the

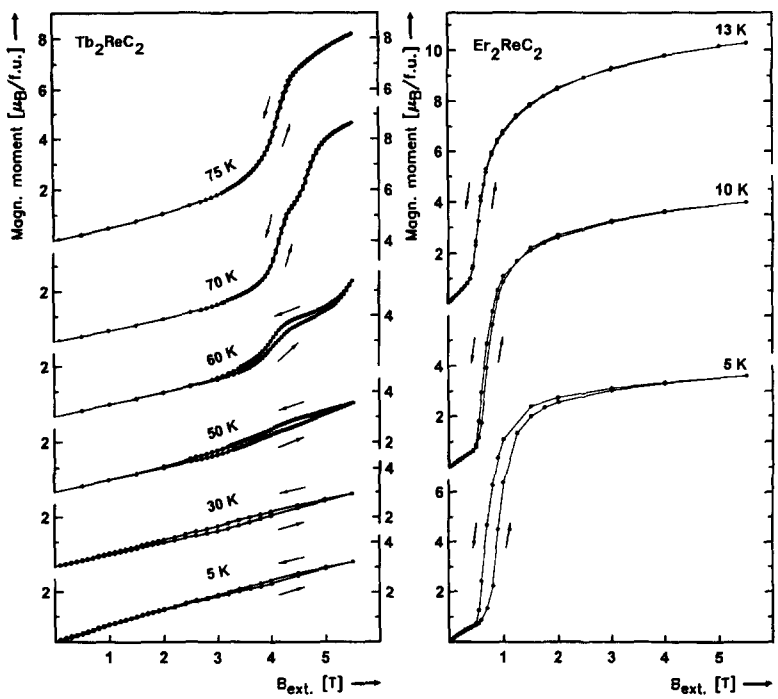

Fig. 3. Hysteresis loops of Tb_2ReC_2 and Er_2ReC_2 at different temperatures.

impurity of metallic rhenium were refined. Residuals (defined as $R_N = \Sigma|F_0 - |F_c||/\Sigma F_0$) of $R_N =$ 0.085 and 0.070 were obtained for the nuclear structures of Tb_2ReC_2 and Er_2ReC_2, respectively. These values seem to be rather high, however, they are acceptable in view of the rather poor counting statistics. The refined atomic positions shown in Table 2 are in good agreement with those of the X-ray data measured at 300 K [19].

In a band structure calculation for the Ln_2ReC_2 carbides, using the extended Hückel method, and assuming a complete transfer from the electropositive lanthanoid atoms to the rhenium–carbon polyanion, it was found that the electrons at the Fermi level occupy antibonding states [20]. To rationalize this somewhat unexpected result, it was suggested that the Pr_2ReC_2 type carbides contain additional atoms at the interstitial site 4b (0, 0, $\frac{1}{2}$). Subsequently the single-crystal X-ray data of Er_2ReC_2 were refined again [27], assuming that site to be occupied by carbon atoms. This refinement – approached slowly with the proper damping – resulted in a slightly negative occupancy factor of $-0.2 \pm 3.7\%$. The highest electron density for another interstitial site in the final difference Fourier analysis amounted to only 16% of the electron density expected for a carbon atom [27].

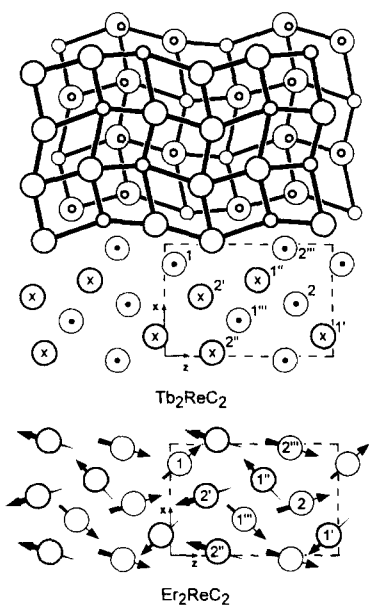

Fig. 4. Nuclear and magnetic structures of Tb_2ReC_2 and Er_2ReC_2. In the upper parts of the drawing the rare-earth, rhenium and carbon atoms are shown as large, medium and small circles. Atoms connected by thin and thick lines are at $y = \frac{1}{4}$ and $y = \frac{3}{4}$, respectively. Some carbon atoms at $y = \frac{1}{4}$ are hidden by rare-earth atoms at $y = \frac{3}{4}$. In the lower part only the lanthanoid atoms with their ordered magnetic moments are shown. In Tb_2ReC_2 the magnetic moments are ordered parallel to the y axis and the moment direction is symbolized with · for spin-up and × for spin-down. The magnetic moments of the erbium atoms are essentially oriented parallell to the xz plane with small tilts up- or down-wards as indicated by the arrows.

It is extremely unlikely that the sample contained hydrogen, because the sample was prepared by arc-melting. Nevertheless, we have now placed carbon and also hydrogen atoms at the 4b site and refined the neutron powder diffraction data recorded at 150 K with this model. This resulted in residuals of more than 20% in both cases. When the occupancy parameters of that site were allowed to vary, occupancies of $4 \pm 2\%$ and $8 \pm 3\%$ were obtained for the carbon and hydrogen atoms, respectively. Thus, there is neither experimental evidence for the occupancy of that site by impurity elements, nor of any other site.

The magnetic reflections appearing at low temperatures for both compounds, can be indexed using the crystallographic cell. As this cell is primitive, a propagation vector $\boldsymbol{k} = (0, 0, 0)$ is characteristic for both magnetic structures. To solve the magnetic structures we have searched systematically the basis functions of the irreducible representations of the space group Pnma for the propagation vector at point Γ of the Brillouin zone. This has been studied in many cases by different authors. The reader may consult one pioneering paper of this method by Bertaut [28] for the same space group in the setting Pbnm. In our case we use the following numbering for the different sublattices of the Wyckoff position 4c of the symmetry $\cdot m \cdot$ of Pnma: (1) x, $\frac{1}{4}$, z; (2) $-x$, $\frac{3}{4}$, $-z$; (3) $\frac{1}{2} - x$, $\frac{3}{4}$, $\frac{1}{2} + z$; (4) $\frac{1}{2} + x$, $\frac{1}{4}$, $\frac{1}{2} - z$.

The basis functions of the irreducible representations describing possible magnetic structures can be written in terms of linear combinations of the magnetic moments attached to the above positions. We use here the notation of Ref. [28] for the following sequences of + and − signs: F(+ + + +), G(+ − + −), C(+ + − −) and A(+ − − +). A basis function like G_x describes a magnetic structure in which the x component of the magnetic moments

on the four sublattice sites are related by the following equations: $m_{x2} = -m_{x1}$, $m_{x3} = m_{x1}$, $m_{x4} = -m_{x1}$. Table 3 shows the eight one-dimensional irreducible representations of Pnma for the Γ point of the Brillouin zone ($k = 0$). The presence of a mirror plane in the point symmetry of the 4c site has as a consequence the splitting of the possible magnetic structures (basis functions) in two sets: the first one, hereafter called S1, formed by moment arrangements parallel to the b axis (perpendicular to the mirror plane) and the second one, hereafter called S2, constituted by moment arrangements within the mirror plane.

In our case we have two crystallographic positions for the rare-earth elements and, in principle, the atoms of these two sites need not be related by any symmetry relation. In general, when the interaction between the sublattices of the two sites is strong, the magnetic ordering of both sets belongs to the same irreducible representation [28]. However, as stated by Izyumov and coworkers [29–32], the magnetic structures found in about 10% of the data collected in Ref. [33] should be described by a 'reducible' (mixture of at least two ireps) representation. Bertaut [28] has shown that this mixture can occur only if the basis functions are orthogonal for a Hamiltonian of second order. This corresponds to a lowering of the symmetry: the magnetic space group belongs to another 'family' in the sense of the Opechowski–Guccione terminology [34].

Considering the two 4c sublattices, one can easily show that the components $F_{M\alpha}$ ($\alpha = x, y, z$) of the magnetic structure factors corresponding to the reflections ($h00$), ($0k0$) and ($00l$) satisfy simple reflection conditions for each mode F, G, C and A: $F_{M\alpha}$ ($h00$) = 0 for A and F modes if $h = 2n + 1$, and for C and G modes if $h = 2n$; $F_{M\alpha}$ ($0k0$) = 0 for G and C modes whatever k, and for A if $k = 2n$, and for F if $k = 2n + 1$; $F_{M\alpha}$ ($00l$) = 0 for F and G modes if $l = 2n + 1$, and for A and C modes if $l = 2n$.

In applying these conditions one has to keep in mind that the magnetic intensity is proportional to the perpendicular projection of the scattering vector of the total magnetic structure factor. Hence, only

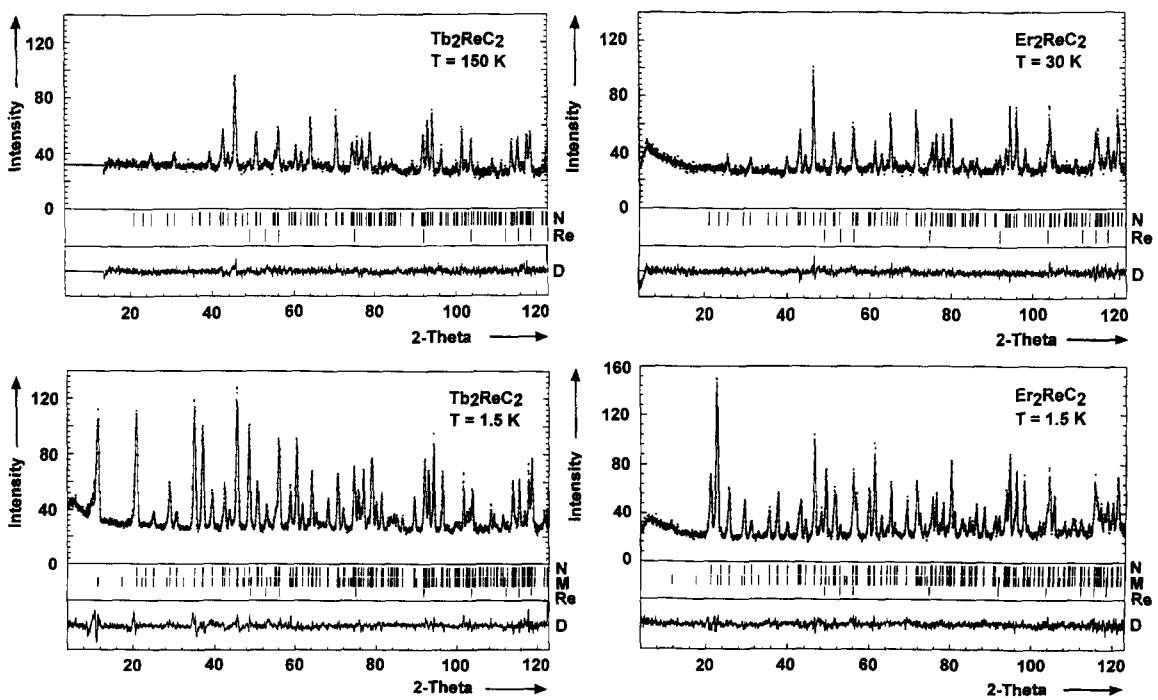

Fig. 5. Neutron diffraction patterns of Tb_2ReC_2 and Er_2ReC_2. The peak positions of the nuclear (N) and the magnetic (M) structures and the impurity of metallic rhenium as well as the differences (D) between the observed and calculated patterns are shown.

Table 2
Results of the Rietveld refinements of the neutron powder diffraction data ($\lambda = 198.5$ pm) for the nuclear structures of the orthorhombic carbides Tb_2ReC_2 and Er_2ReC_2. The atomic parameters at 300 K for both compounds are taken from the X-ray data of Ref. [19]. All atoms are at the position 4c (x, $\frac{1}{4}$, z) of space group Pnma. The isotropic thermal parameters B are given in 10^4 pm^2; R_N is the residual of the nuclear structure with the number of structure factors in parentheses

	Tb_2ReC_2			Er_2ReC_2		
	1.5 K	150 K	300 K	1.5 K	30 K	300 K
a [pm]	655.19(3)	655.23(4)	655.85(6)	649.99(3)	649.76(4)	649.90(8)
b [pm]	511.76(2)	512.36(3)	512.92(6)	502.97(2)	503.03(3)	503.53(2)
c [pm]	985.19(4)	985.75(6)	986.8(1)	972.45(5)	973.06(6)	974.31(9)
V [nm^3]	0.33033	0.33093	0.3319	0.31792	0.31804	0.3188
x (Ln1)	0.816(1)	0.812(1)	–	0.821(1)	0.819(1)	0.82071(8)
z (Ln1)	0.0541(6)	0.0531(8)	–	0.0591(7)	0.0590(7)	0.05687(4)
x (Ln2)	0.4684(9)	0.466(1)	–	0.463(1)	0.465(1)	0.46535(7)
z (Ln2)	0.7874(6)	0.7875(9)	–	0.7853(9)	0.7846(8)	0.78329(5)
x (Re)	0.278(1)	0.277(1)	–	0.286(1)	0.284(1)	0.28201(6)
z (Re)	0.1343(6)	0.1344(6)	–	0.1276(8)	0.1298(7)	0.13120(4)
x (C1)	0.043(2)	0.045(2)	–	0.046(2)	0.045(2)	0.048(2)
z (C1)	0.256(1)	0.2580(9)	–	0.261(1)	0.2579(9)	0.260(1)
x (C2)	0.675(2)	0.673(2)	–	0.671(2)	0.669(1)	0.676(2)
z (C2)	0.550(1)	0.550(1)	–	0.555(1)	0.5532(9)	0.5537(9)
B (Ln1)	0.45(8)	0.3(2)	–	0.3(1)	0.4(2)	0.553(6)
B (Ln2)	0.40(8)	0.9(2)	–	0.7(1)	0.9(2)	0.591(7)
B (Re)	0.5(2)	0.8(1)	–	0.3(2)	0.3(1)	0.491(6)
B (C1)	0.9(2)	0.2(2)	–	0.6(2)	0.5(2)	0.7(1)
B (C2)	0.9(2)	1.0(2)	–	1.0(3)	0.2(2)	0.5(1)
R_N	0.060 (138)	0.085 (139)	–	0.039 (136)	0.070 (136)	0.032 (842)

the components yz, xz and xy contribute to the reflections ($h00$), ($0k0$) and ($00l$), respectively. In following these conditions, it is possible to decide from the observed (and unobserved) magnetic intensities which representation of the table is to be used, and one can start with the magnetic structure refinement within the symmetry constraints imposed by the corresponding basis functions.

Table 3
Irreducible representations of Pnma for $\boldsymbol{k} = 0$. The basis functions corresponding to the Wyckoff position 4c of symmetry $\cdot m \cdot$ can easily be obtained by applying the projection operator technique to the corresponding magnetic moment component. The Shubnikov magnetic group symbol is also shown. The two signs + and − correspond to the characters +1 and −1 of the generators 2_{1y} (0, y, 0) and 2_{1z} ($\frac{1}{4}$, 0, z). The subscripts 'g' and 'u' correspond to the characters +1 (gerade) or −1 (ungerade) of the inversion with respect to the origin (third generator)

Representation	Basis functions			Shubnikov group
Γ_{1g} (+ +)	–	C_y	–	Pnma
Γ_{2g} (− +)	C_x	–	F_z	Pn′m′a
Γ_{3g} (+ −)	–	F_y	–	Pn′ma′
Γ_{4g} (− −)	F_x	–	C_z	Pnm′a′
Γ_{1u} (+ +)	A_x	–	G_z	Pn′m′a′
Γ_{2u} (− +)	–	A_y	–	Pnm′a
Γ_{3u} (+ −)	G_x	–	A_z	Pnma′
Γ_{4u} (− −)	–	G_y	–	Pn′ma

We shall start discussing the more simple case of Tb_2ReC_2. The analysis of the magnetic reflections gives the following set of observations: ($h00$) reflections are observed and intense only when h is even, ($0k0$) reflections are not observed, and ($00l$) reflections are observed and intense only when l is odd. The absence of the ($0k0$) reflections suggests the presence of the modes G or C, or it may also indicate that the magnetic ordering belongs to the set S1. Adding the other conditions leads to the unambiguous identification of a mode A along the b axis. This corresponds to the representation Γ_{2u} (− +) with the basis function [0, A_y, 0] for the two terbium sites. The magnetic structure can then be described by the composed basis function [0, $A_y^{(1)} + A_y^{(2)}$, 0]. The magnetic space group in this case is Pnm′a.

In the case of Er_2ReC_2 the situation is much more complicated. The reflection conditions are the fol-

lowing: $(h00)$ only observed for $h = 2n$, $(0k0)$ observed and intense for k = odd ($k = 1, 3$) and $(00l)$ very weak, but observed for l odd or even. At variance with the case of the terbium compound, the observation of intense $(0k0)$ reflections indicates that the moments are in a first approximation perpendicular to the b axis. Thus the magnetic structure must belong to the set S2. The first condition suggests the presence of the modes A or F, and the second one suggests the presence of a mode A and not a mode F. The third condition – concerning the reflections $(00l)$ – indicates that there may be a mixture of representations, because no selection rule is observed for these reflections. Due to the weakness of the (001) reflection we can ignore its existence for a first trial. The other conditions suggest either the representation $\Gamma_{1u}(++)$ [A_x, 0, G_z] or $\Gamma_{3u}(+-)$ [G_x, 0, A_z] as possible descriptions of the magnetic structure. Trials of the Γ_{1u} representation gave always very poor R values and a too high intensity for the (001) reflection, as expected from the fact that the mode A_x gives zero intensity for $(00l)$ reflections only when $l = 2n$. The refinement within the $\Gamma_{3u}(+-)$ representation, for both sites, gave essentially correct results. However, zero intensity is calculated for the reflection (001) as expected for a G_x mode (the A_z mode does not contribute to the $(00l)$ reflections). If we take into account the small (001) reflection, another representation from the set S1 should be considered. Only the modes C_y and A_y are compatible with the presence of the (001) reflection. The introduction of these components into the refinement model converged only for the A_y mode. Then the magnetic structure can be described by a reducible representation $\Gamma = \Gamma_{2u} \oplus \Gamma_{3u}$ with basis functions [G_x, A_y, A_z] for both sites. In refining these models by varying the orientation and the magnitude of the magnetic moments of both erbium sites, we immediately obtained the results which are summarized in Table 4 for the magnetic structure and in Table 2 for the nuclear structure. For the magnetic structures the residuals $R_M = 0.055$ and 0.062 were obtained for the terbium and erbium sublattices, respectively. Because of the better counting statistics of the 1.5 K data sets the residuals $R_N = 0.060$ and 0.039 for the nuclear structures of Tb_2ReC_2 and Er_2ReC_2 are lower than the residuals for the refinements of the high temperature data.

In the case of the terbium compound we had collected three data sets at the temperatures 1.5, 50 and 80 K using the wavelength 311 pm and two data sets at 1.5 and 150 K with the wavelength 198.5 pm. As already mentioned, the nuclear structure was refined only from the data collected with the wavelength 198.5 pm. For the refinements with the longer wavelength the nuclear structure was fixed at the values obtained with the shorter wavelength and only the magnetic structure was refined. The results obtained for the magnetic structures from all data sets are summarized in Table 4. It can be seen that the results for Tb_2ReC_2 obtained for 1.5 K with the two different wavelengths are in good agreement. With

Table 4
Results of the Rietveld refinements of the neutron powder data of the orthorhombic carbides Ln_2ReC_2 (Ln = Tb and Er). The experimental moments in units of μ_B at the given temperatures are compared with those of the theoretical values $\mu_s = gJ\ \mu_B$ of the free R^{3+} ions. The residuals for the magnetic structures R_M, are listed together with the corresponding number of structure factors in parentheses.

	Tb_2ReC_2	Tb_2ReC_2	Tb_2ReC_2	Tb_2ReC_2	Er_2ReC_2
λ [pm]	198.5	311	311	311	198.5
T [K]	1.5	1.5	50	80	1.5
μ_x (Ln1)	0	0	0	0	4.83(8)
μ_y (Ln1)	8.17(5)	8.17(4)	6.00(3)	3.84(3)	0.37(15)
μ_z (Ln1)	0	0	0	0	5.27(9)
μ_{tot} (Ln1)	8.17(5)	8.17(4)	6.00(3)	3.84(3)	7.16(11)
μ_x (Ln2)	0	0	0	0	2.03(11)
μ_y (Ln2)	8.01(5)	8.34(4)	8.07(3)	6.50(3)	1.03(12)
μ_z (Ln2)	0	0	0	0	7.33(10)
μ_{tot} (Ln2)	8.01(5)	8.34(4)	8.07(3)	6.50(3)	7.68(11)
μ_s (Ln^{3+})	9.00	9.00	9.00	9.00	9.00
R_M (no. of F's)	0.055 (136)	0.054 (43)	0.054 (43)	0.055 (43)	0.062 (161)

increasing temperature the ordered components of the magnetic moments of both terbium sites decrease, and it can be expected that they disappear at the Néel temperature of 96(2) K, obtained from the magnetic susceptibility data. The magnetic moment observed for the Tb1 site decreases more rapidly than that for the Tb2 site. Even though other refinement models were tried for the data sets of 50 and 80 K, the orientation of the moments for the two sites remained parallel to the y axis. The complicated topology of the magnetic lattice and the absence of models for the exchange interactions in these carbides makes it difficult to rationalize the different temperature behaviour of the magnetic order of the Tb1 and Tb2 moments. However, it is clear that the number of terbium neighbours for the two terbium sites is different [19], and for that reason it is not surprising that they have different magnetic ordering behaviour.

In the erbium compound the magnetic moments are almost perpendicular to the y axis (Fig. 4), i.e. the μ_y components of the magnetic moments are very small (Table 4). The resulting total moments for the two erbium sites of $\mu_{tot}(Er1) = 7.16(11)\mu_B$ and $\mu_{tot}(Er2) = 7.68(11)\mu_B$ are smaller than the corresponding moments $\mu_{tot}(Tb1) = 8.17(4)\mu_B$ and $\mu_{tot}(Tb2) = 8.34(4)\mu_B$ and also smaller than the maximum possible theoretical moments of $\mu_s = g\,J\,\mu_B = 9.0\mu_B$ which are the same for both, erbium and terbium. Listings of the observed and calculated structure factors are available [35].

The reason for the different magnetic structures is, as in many other rare-earth systems, the different single ion anisotropy term (characteristic of the rare-earth ion in a particular crystal field) in the Hamiltonian governing the magnetic ordering. From the magnetic structures can be deduced that the Tb^{3+} ions have strong uniaxial anisotropy (Ising-like behaviour), whereas the Er^{3+} ions behave closely to an XY Heisenberg antiferromagnet.

Acknowledgements

We are grateful to Dr. H.G. Nadler (H.C. Starck Co) and Dr. G. Höfer (Heraeus Quarzschmelze) for generous gifts of rhenium powder and silica tubes. This work was supported by the Deutsche Forschungsgemeinschaft and the Fonds der Chemischen Industrie.

References

[1] A. Paoluzi, G. Turilli, O. Moze and F. Licci, eds., Procs. 3rd Eur. Magnetic Materials and Applications Conf., Sept. 1989, Rimini, J. Magn. Magn. Mater. 83 (1990).
[2] S. Kobe and S. Roth, eds., Procs. 4th Eur. Magnetic Materials and Applications Conf., April 1991, Dresden, J. Magn. Magn. Mater. 101 (1991).
[3] S.B. Palmer, ed., Procs. Int. Conf. on Magnetism, Sept. 1991, Edinburgh, J. Magn. Magn. Mater. 104–107 (1992).
[4] R.-D. Hoffmann, W. Jeitschko, M. Reehuis and S. Lee, Inorg. Chem. 28 (1989) 934.
[5] R.-D. Hoffmann, W. Jeitschko and L. Boonk, Chem. Mater. 1 (1989) 580.
[6] P.A. Kotsanidis, J.K. Yakinthos and E. Gamari-Seale, J. Less-Common Met. 152 (1989) 287.
[7] U.E. Musanke, R.-D. Hoffmann and W. Jeitschko, Z. Kristallogr. 205 (1993) 201.
[8] K. Zeppenfeld, R. Pöttgen, M. Reehuis, W. Jeitschko and R.K. Behrens, J. Phys. Chem. Solids 54 (1993) 257.
[9] U.E. Musanke, W. Jeitschko and M.E. Danebrock, Z. Anorg. Allg. Chem. 619 (1993) 321.
[10] G.E. Kahnert and W. Jeitschko, J. Alloys & Comp. 196 (1993) 199.
[11] W. Schäfer, G. Will, J.K. Yakinthos and P.A. Kotsanidis, J. Magn. Magn. Mater. 88 (1990) 13.
[12] M.E. Danebrock, W. Jeitschko, A.M. Witte and R. Pöttgen, J. Phys. Chem. Solids 56 (1995) 807.
[13] W. Schäfer, G. Will, J.K. Yakinthos and P.A. Kotsanidis, J. Alloys & Comp. 180 (1992) 251.
[14] J.K. Yakinthos, P.A. Kotsanidis, W. Schäfer and G. Will, J. Magn. Magn. Mater. 81 (1989) 163.
[15] J.K. Yakinthos, P.A. Kotsanidis, W. Schäfer and G. Will, J. Magn. Magn. Mater. 89 (1990) 299.
[16] J.K. Yakinthos, P.A. Kotsanidis, W. Schäfer and G. Will, J. Magn. Magn. Mater. 102 (1991) 71.
[17] W. Schäfer, W. Kockelmann, G. Will, P.A. Kotsanidis, J.K. Yakinthos and J. Linhart, J. Magn. Magn. Mater. 132 (1994) 243.
[18] M. Reehuis, K. Zeppenfeld and W. Jeitschko, J. Alloys & Comp. 209 (1994) 217.
[19] W. Jeitschko, G. Block, G.E. Kahnert and R.K. Behrens, J. Solid State Chem. 89 (1990) 191.
[20] H. Deng and R. Hoffmann, Inorg. Chem. 32 (1993) 1991.
[21] J. Rodriguez-Carvajal, FULLPROF: A Program for Rietveld Refinement and Profile Matching Analysis of Complex Powder Diffraction Patterns; Institut Laue–Langevin (1991) unpublished.
[22] V.F. Sears, Atomic Energy of Canada Limited, AECL-8490 (1984).
[23] P.J. Brown, Magnetic Form Factors, in: International Tables for Crystallography, ed. A.J.C. Wilson, Vol. C (Kluwer Academic, Dordrecht, 1992) p. 391.

[24] K. Hiebl, C. Horvath, P. Rogl and M.J. Sienko, J. Magn. Magn. Mater. 37 (1983) 287.
[25] M. Slaski, A. Szytuła, J. Leciejewicz and A. Zygmunt, J. Magn. Magn. Mater. 46 (1984) 114.
[26] T. Shigeoka, N. Iwata and H Fujii, J. Magn. Magn. Mater. 104–107 (1992) 1229.
[27] G.E. Kahnert and W. Jeitschko (1993) unpublished results.
[28] E.F. Bertaut, Acta Crystallogr. A 24 (1968) 217; see also J. de Phys. Coll. C1 32 (2–3) (1971) 462 and J. Magn. Magn. Mater. 24 (1981) 267.
[29] Y.A. Izyumov and V.E. Naish, J. Magn. Magn. Mater. 12 (1979) 239.
[30] Y.A. Izyumov, V.E. Naish and V.N. Syromiatnikov, J. Magn. Magn. Mater. 12 (1979) 249.
[31] Y.A. Izyumov, V.E. Naish and S.B. Petrov, J. Magn. Magn. Mater. 13 (1979) 267; ibid. 13 (1979) 275.
[32] Y.A. Izyumov, J. Magn. Magn. Mater. 21 (1980) 33.
[33] A. Oleś, F. Kajzar, M. Kucab and W. Sikora, in: Magnetic Structures Determined by Neutron Diffraction (Panstwowe Wydawnictwo Naukowe, Warszawa, 1976).
[34] W. Opechowski and R. Guccione, Magnetic Symmetry, in: Magnetism, eds. G.T Rado and H. Suhl, Vol. II A (Academic Press, New York, 1965) ch. 3 p. 105.
[35] M.E. Danebrock, Ph.D. Thesis, Universität Münster (1994).